

SAND REPORT

SAND2003-2007
Unlimited Release
Printed June 2003

Chem-Prep PZT 95/5 for Neutron Generator Applications: Powder Fractionation Study of Production-Scale Powders

Diana L. Moore, James A. Voigt, Chad S. Watson, Bonnie B. McKenzie, Roger H. Moore, Michael A. Hutchinson, Steven J. Lockwood, and Emily D. Rodman

Prepared by
Sandia National Laboratories
Albuquerque, New Mexico 87185 and Livermore, California 94550

Sandia is a multiprogram laboratory operated by Sandia Corporation, a Lockheed Martin Company, for the United States Department of Energy under Contract DE-AC04-94AL85000.

Approved for public release; further dissemination unlimited.



Sandia National Laboratories

Issued by Sandia National Laboratories, operated for the United States Department of Energy by Sandia Corporation.

NOTICE: This report was prepared as an account of work sponsored by an agency of the United States Government. Neither the United States Government, nor any agency thereof, nor any of their employees, nor any of their contractors, subcontractors, or their employees, make any warranty, express or implied, or assume any legal liability or responsibility for the accuracy, completeness, or usefulness of any information, apparatus, product, or process disclosed, or represent that its use would not infringe privately owned rights. Reference herein to any specific commercial product, process, or service by trade name, trademark, manufacturer, or otherwise, does not necessarily constitute or imply its endorsement, recommendation, or favoring by the United States Government, any agency thereof, or any of their contractors or subcontractors. The views and opinions expressed herein do not necessarily state or reflect those of the United States Government, any agency thereof, or any of their contractors.

Printed in the United States of America. This report has been reproduced directly from the best available copy.

Available to DOE and DOE contractors from
U.S. Department of Energy
Office of Scientific and Technical Information
P.O. Box 62
Oak Ridge, TN 37831

Telephone: (865)576-8401
Facsimile: (865)576-5728
E-Mail: reports@adonis.osti.gov
Online ordering: <http://www.doe.gov/bridge>

Available to the public from
U.S. Department of Commerce
National Technical Information Service
5285 Port Royal Rd
Springfield, VA 22161

Telephone: (800)553-6847
Facsimile: (703)605-6900
E-Mail: orders@ntis.fedworld.gov
Online order: <http://www.ntis.gov/ordering.htm>



SAND2003-2007
Unlimited Release
Printed June 2003

Chem-Prep PZT 95/5 for Neutron Generator Applications: Powder Fractionation Study of Production-Scale Powders

Diana L. Moore, James A. Voigt
Chemical Synthesis and Nanomaterials Department

Chad S. Watson
Ceramic Materials Department

Bonnie B. McKenzie
Materials Characterization Department

Roger H. Moore, Michael A. Hutchinson, Steven J. Lockwood, Emily D. Rodman
Ceramic and Glass Department

Sandia National Laboratories
P.O. Box 5800
Albuquerque, NM 87185-1411

Abstract

The Materials Chemistry Department 1846 has developed a lab-scale chem-prep process for the synthesis of PNZT 95/5, referred to as the “SP” process (Sandia Process). This process (TSP) has been successfully transferred to and scaled-up by Department 14192 (Ceramics and Glass Department), producing the larger quantities of PZT powder required to meet the future supply needs of Sandia for neutron generator production. The particle size distributions of TSP powders routinely have been found to contain a large particle size fraction that was absent in development (SP) powders. This SAND report documents experimental studies focused on characterizing these particles and assessing their potential impact on material performance. To characterize these larger particles, fractionation of several TSP powders was performed. The “large particle size fractions” obtained were characterized by particle size analysis, SEM, and ICP analysis and incorporated into compacts and sintered. Large particles were found to be very similar in structure and composition as the bulk of the powder. Studies showed that the large-size fractions of the powders behave similarly to the non-fractionated powder with respect to the types of microstructural features once sintered. Powders were also compared that were prepared using different post-synthesis processing (i.e. differences in precipitate drying). Results showed that these powders contained different amounts and sizes of porous inclusions when sintered. How this affects the functional performance of the PZT 95/5 material is the subject of future investigations.

Acknowledgements

The authors would like to acknowledge Ted Montoya and Tom Spindle for the powder processing and sintering work; Jeanne Barrera, Polly Wilks, and Jeff Reich for ICP compositional analysis of the powders; and the Department 1822 Metallography lab for the sample preparation for SEM analysis.

Contents

Abstract.....	3
Acknowledgements.....	4
Introduction.....	9
Methods.....	10
Powder Synthesis.....	10
Particle Size Measurement.....	10
Experimental.....	10
Study #1: Comparison of SP and TSP Produced Powders	10
“Large-Size Fraction”	11
“Middle-Size Fraction”	11
“Fines-Size Fraction”	12
SP16O	12
Study #2: Large-Scale Fractionation of TSP-46.....	12
“Large-Size Fraction”	13
Study #3: Effects of Large-Size Fraction on Sintering.....	13
Results and Discussion	15
Study #1: Comparison of SP and TSP Produced Powders	15
Study #2: Large-Scale Fractionation of TSP-46.....	16
PSD Analysis of the Large-size Fraction as a Powder	16
PSD Analysis of the Large-size Fraction as a Slurry.....	17
Study #3: Effects of Large-Size Fraction on Sintering.....	18
Conclusions.....	21
References.....	34

Figures

Figure 1. Comparison of PSD of SP16 Series powders to TSP Center Point (CP) batch powders	22
Figure 2. Overlay of PSD curves for three size fractions of TSP-46 compared to the non-fractionated TSP 46 powder	22
Figure 3. Overlay of PSD curves for three size fractions of SP16O compared to the non-fractionated SP16O powder.....	23
Figure 4. SEM photomicrographs of TSP 46 fines-size fraction and large-size fraction	23
Figure 5. SEM photomicrograph of large-size fraction of TSP-46 showing the rounded morphology of the agglomerates that are comprised of the sub-micron PZT primary Particles.....	24
Figure 6. SEM photomicrograph of fines-size fraction of SP16O showing PZT primary particles equivalent to those seen in the fines-size fraction of TSP46.....	24

Figure 7. Particle size distribution data of TSP-46 large-size fraction analyzed as a powder rather than as a slurry	25
Figure 8. PSD overlays of TSP-46 large-size fraction as a function of increasing sonication times of slurry sample prior to particle size analysis	25
Figure 9. SEM photomicrograph of agglomerate cross-section of encapsulated and polished loose powder from large-size fraction of TSP-46	26
Figure 10. High magnification SEM photomicrographs of agglomerate cross-section of encapsulated and polished loose powder from large-size fraction of TSP-46	26
Figure 11. PSD of non-fractionated TSP-59 and TSP-60 powders showing the volume % of particles > ~10 μm	27
Figure 12. SEM photomicrograph of agglomerate cross-section of encapsulated and polished loose powder from large-size fraction of TSP-59	27
Figure 13. Higher magnification SEM photomicrograph of agglomerate cross-section of encapsulated and polished loose powder from large-size fraction of TSP-59	28
Figure 14. SEM photomicrograph of agglomerate cross-section of encapsulated and polished loose powder from large-size fraction of TSP-60	28
Figure 15. Higher magnification SEM photomicrograph of agglomerate cross-section of encapsulated and polished loose powder from large-size fraction of TSP-59	29
Figure 16. 95% confidence intervals for ICP compositional analyses of Nb for the TSP-59 and TSP-60 series powders.....	29
Figure 17. 96% confidence intervals for ICP compositional analyses of Zr for the TSP-59 series powders.....	30
Figure 18. 95% confidence intervals for ICP compositional analyses of Zr for the TSP-60 series powders.....	30
Figure 19. 95% confidence intervals for ICP compositional analyses of Pb for the TSP-59 and TSP-60 series powders.....	31
Figure 20. Schematic to illustrate the method of layering large-size fraction powder between layers of a TSP powder blend to form a slug for high fire	31
Figure 21. SEM photomicrographs of polished cross-sections of the large-size fraction layers comprised of powders TSP-59 and TSP-60 in high fired slugs.....	32

Figure 22. Higher magnification SEM photomicrographs of polished cross-sections of the large-size fraction layers comprised of powders TSP-59 and TSP-60 in high fired slugs.....	32
---	----

Figure 23. SEM photomicrographs of polished cross-sections of slugs prepared from non-fractionated powders of TSP-59 and TSP-60	33
---	----

Figure 24. SEM photomicrographs of polished cross-sections of slugs prepared from powders TSP-58 and TSP-61	33
---	----

Tables

Table 1. Particle Size Results for Large-size Fraction and Non-fractionated TSP-46 Powder as a Function of Sonication Time	17
--	----

Table 2. ICP Results for Non-fractionated and Large-size Fractions of TSP-59 and TSP-60	19
---	----

Intentionally Left Blank

Chem-Prep PZT 95/5 for Neutron Generator Applications: Powder Fractionation Study of Production-Scale Powders

Introduction

The Chemical Synthesis and Nanomaterials Department (1846) has developed a lab-scale chem-prep process¹ for the synthesis of PNZT 95/5, a ferroelectric material that is used in neutron generator power supplies. This process (Sandia Process or SP) has been successfully transferred (Transferred Sandia Process or TSP) to and scaled by Department 14192 (Ceramics and Glass Department) to meet the future supply needs of Sandia for its neutron generator production responsibilities.

In going from the development-size SP batch (1.6 kg/batch) to the production-scale TSP powder batch size (10 kg/batch), it was important to determine if the scaling process caused any changes in material properties that could lead to “performance-critical” changes in the functional properties of PNZT 95/5. One area where a difference was found between the SP and TSP processes was in the particle size distributions of their respective calcined PNZT powders. A comparison of the particle size distribution of SP- and TSP-derived powders showed that the TSP powders tend to have a “tail” in the distribution (volume fraction of particles $> \sim 10\mu\text{m}$) that was absent for the SP powders (Figure 1). The particle size distribution (PSD), as well as compositional homogeneity of a powder, can play a role in the powders’ subsequent densification, electrical response, and functional properties. Efforts to determine the origin of these larger particles is reported elsewhere². This report documents fractionation studies (isolation of large particles) performed to better characterize the large-size fraction of the powder and to determine its potential impact, if any, on the microstructure and homogeneity of sintered PNZT 95/5 ceramics.

The powder fractionation method was modeled after the approach used to prepare samples for routine particle size distribution analysis (details given below). As the work evolved, three fractionation studies were ultimately performed. For the initial study, scanning electron microscopy (SEM) characterization and particle size distribution analyses were performed on the powder particle size fractions obtained from a production-scale powder (TSP-46) and a development-scale powder (SP16O). To isolate a larger quantity of the “large-size fraction” of the TSP powder for more detailed PSD analysis and SEM characterization, a second fractionation study was performed. Finally, a sintering study to determine the effect large particles may have on the final ceramic microstructure of PNZT 95/5 was carried out.

Methods

Powder Synthesis

The production-scale chemical synthesis of the TSP powders is documented elsewhere³. Specific powder preparation details relevant to these studies will be discussed as appropriate.

Particle Size Measurement

The particle size distribution for powders described in this report were determined on calcined powders (900°C for 16 hours) using a Coulter Model LS230 particle size analyzer. Sample preparation involved using a 50 mg aliquot of the powder, wetted with 2 drops of Darvan 821A dispersant (R.T. Vanderbilt, 40% solution) to form a fluid paste, and then diluted with 20 mL of degassed, filtered (0.2 µm) tap water. The slurry was both stirred and ultrasonically dispersed simultaneously (Heat Systems Model W375 sonicator, with a 1/4 inch micro tip, operated at 50% duty cycle and 50% power) for three minutes prior to analysis. An aliquot of this slurry was then introduced into the Coulter sample cell for the analysis. Three PSDs were obtained per aliquot, and a representative plot is presented in this report. To repeat an analysis, a fresh slurry sample was prepared as just described.

Experimental

Study #1: Comparison of SP and TSP Produced Powders

Powder TSP-46 (10 kg) was synthesized at 0.5% excess Pb with a Zr/Ti ratio of 95.5/4.5. The post-precipitation, or “post-synthesis” processing conditions consisted of vacuum filtration of the powder in two 24 inch diameter filters (lined with Whatman No. 3 ashless filter paper) for six days (manual break-up of the filter cake twice daily on days 1, 2, 5 and 6 after synthesis) followed by oven drying for 33 hours in eight 9 x 13 x 2 inch Pyrex trays (88°C, Hotpack drying oven, Model 217602-4). The oven-dried oxalate powder was pyrolyzed for 16 hours at 400°C with 150 scfm air flow (Lindberg Treet-All box furnace, Model 11-MT-183618-21AM), then ball milled for 15 hours in two 15 liter plastic carboys each containing 38 pounds of half-inch ZrO₂ media. The media and powder were separated using a CSC Scientific Sieve Shaker utilizing a stacked array of sieves (U.S.A. Standard Sieve, ASTM) at an intensity setting of 3 for 3 minutes per sieve loading. The powder plus media were placed into two No. 4 sieves (4.8 mm opening) stacked upon a No. 20 sieve (850 µm opening); the +20 mesh fraction was captured and isolated from the powder fraction collected for calcination. Calcination was done at 900°C for 16 hours (covered crucibles, no air flow) in the Lindberg Treet-All furnace.

This fractionation study was modeled directly after the sample preparation method used when preparing slurries for particle size analysis. A 1.00 g TSP-46 quantity of powder

was wetted with 40 drops of Darvan 821A and mixed to form a paste, to which 20 mL of DI water was added. This slurry was ultrasonically dispersed as described in the particle size characterization overview section. The slurry was poured into a 250 mL graduated cylinder containing 200 mL DI water. The total volume of the slurry, with beaker rinses, was ~232 mL.

"Large-Size Fraction"

After ~4 minutes of settling time, the suspension was pumped from the cylinder, first at ~220 mL/minute, then increased to ~260 mL/minute (Cole Parmer Pump Model 7523-20, Cole Parmer Pump Head Model 7518-10, Tygon tubing 6409-25). After pumping, about 5 mL of slurry was left in the cylinder. This quantity was transferred to a 20 mL glass vial with rinsing (rinses of the cylinder also were collected; it was noted that there were still large particles uncollected from the bottom of the cylinder). This "large-size fraction" was further fractionated by pipetting off the cloudy suspension, adding water, shaking to re-suspend the slurry, and pipetting off the cloudy suspension. This procedure was repeated 3 times, with the third "wash" remaining fairly clear. The resulting slurry was vacuum filtered (0.2 μ m filter, PALL Gelman GH Polypro), and the powder washed on the filter five times with 5 mL aliquots of DI water. The powder was allowed to air dry on the filter overnight. From this quantity of powder, samples for SEM and particle size analysis were prepared:

- SEM: A suspension of the powder in ethanol was sonicated in an ultrasonic water bath (Branson B-22-4) for 1 minute; a droplet of this suspension was placed onto a SEM stub and the ethanol allowed to evaporate. SEM photomicrographs were taken at several magnifications of the deposited, loose particles.
- PSD: A suspension of powder and water was well shaken and mixed prior to particle size analysis. The slurry was not sonicated further. No additional dispersant was added.

"Middle- Size Fraction"

The suspension pumped from the graduated cylinder in the large-size fraction step discussed above was allowed to settle in a second container for 7.5 minutes. This suspension was then decanted, leaving settled particles on the bottom of the beaker. A small amount of water was added to this remnant, and the slurry collected as the "middle-size fraction" of the TSP-46 powder. The particle size aliquot was taken from this quantity after the volume was well mixed and shaken (no further sonication or additional dispersant was used). No SEM photomicrographs were obtained on the middle-size fraction powder.

"Fines-Size Fraction"

The decanted suspension from the middle-size fraction step above was well stirred on a stir plate. A 20 mL aliquot of this suspension was collected and designated the "fines-size fraction." Particle size analysis and SEM photomicrographs were obtained:

- SEM: Ten mL of this suspension were filtered (0.2 μ m filter, PALL GH Polypro), with the powder being washed on the filter five times with 5 mL aliquots of DI water. This collected powder was allowed to air dry on the filter overnight. A vial containing a suspension of powder and ethanol was sonicated in an ultrasonic water bath for 1 minute; a droplet of this suspension was placed onto a SEM stub and the ethanol allowed to evaporate. SEM photomicrographs were taken at several magnifications of the deposited particles.
- PSD: The remaining 10 mL of the "fines-size fraction" were used for particle size analysis. The particle size aliquot was taken from this quantity after the volume was well mixed and shaken (no further sonication or additional dispersant was used).

SP16O

In parallel to the first fractionation study of TSP-46, a similar study was done on powder SP16O. The SP powder was a lab-scale (1.6 kg) development batch chem-prep PNZT 95/5 powder prepared as described in a future SAND report⁴. The slurry preparation, using 1.00 g SP16O powder and 40 drops Darvan 821A, as well as the fractionation steps were similar to the TSP-46 preparation described above. Particle size distribution data were obtained on the three slurry fractions of this powder. SEM photomicrographs were taken at several magnifications on the loose powder "fines-size fraction" only (sample preparation as described above).

Study #2: Large-Scale Fractionation of TSP-46

The second fractionation study was conducted to collect a greater quantity of the large-size fraction of TSP-46 powder for a more detailed particle size analysis. The amount of dispersant used was much less than for the first study (0.32 wt.% Darvan 821A based on oxides), and the more rigorous sonication was not used. For sample preparation, 10.14 g of TSP-46 powder was mixed with 0.080 g Darvan 821A and 100 mL DI water. The suspension was stirred on a stir plate for 5 minutes, sonicated in a ultrasonic water bath for 10 minutes, and then stirred for one more minute prior to being added to a 500 mL graduated cylinder containing 300 mL DI water. The total volume, with beaker rinses, was 450 mL.

"Large-Size Fraction"

After 4 minutes of settling time in the graduated cylinder, the supernatant was pumped off at 300 mL/minute, leaving ~15 mL of slurry in the cylinder. This remaining quantity was transferred to a 125 mL jar using 100 mL DI water. This large-size fraction was further fractionated by pipetting off the cloudy suspension, adding water, shaking to re-suspend the slurry, and pipetting the cloudy suspension. This procedure was done ~7 times. The powder in the jar was dried for ~2 hours at 177°C to 195°C (Fisher Isotemp 500 Series Oven). About 12.4% of the starting powder (1.26 g) was collected as the "large-size fraction." This fraction was analyzed for PSD using two sample preparation methods as outlined below.

- PSD – "Loose Powder" Analysis: The large-size fraction powder was analyzed for PSD as a "loose powder" (the dry powder was added directly to ~125 mL of water in the Coulter LS230 cell without preparation as a slurry) in an attempt to view the size distribution without deagglomerating the particles as routinely occurs by the slurry sample preparation method.
- PSD – "Slurry" Analysis: A second study was conducted to determine the relative strength of the agglomerates of the large-size fraction. Slurries were prepared (as described per Particle Size Characterization Overview) using sonication times of 3, 10, 15, and 30 minutes to determine the change in the PSD as a function of sonication time.
- SEM: Polished "Loose-Powder" Mounts: The large-size fraction was prepared for SEM by encapsulating loose powder in epoxy and polishing.

Study #3: Effects of Large Particles on Sintering

To evaluate the effects the large particles may have on microstructure, two slugs containing a layer of large-size fraction powder sandwiched between layers of non-fractionated powder were prepared. For this study, two TSP powders (TSP-59 and TSP-60) were selected. These powders were prepared using two different post-synthesis processing conditions (filtering and oven-drying). The large-size fractions from the two powders were "layered" between granulated/bindered TSP powder (two separate slugs) and processed as per nominal slug processing (nominal bisque fire schedule of 750°C for 4 hours, and high fire schedule of 1350°C for 6 hours). These slugs were included in a large high fire run (approximately 50 slugs using the standard large rectangular double crucible configuration).

Powder TSP-59 was synthesized at 0.5% excess Pb with a Zr/Ti ratio of 95.7/4.3. The post-synthesis processing conditions consisted of vacuum filtration of the powder in two 24 inch diameter filters for six days (lined with Whatman No. 3 ashless filter paper) (with manual break-up of the filter cake twice daily on days 1, 2, 5 and 6 after synthesis), followed by oven-drying for 32 hours in ten Pyrex trays (88°C, Blue M Friction Aire

oven, Model HS-3802-G). The oven-dried oxalate powder was pyrolyzed, ball milled and calcined as described for TSP-46. The fractionation of this powder is outlined below.

- A mixture of 0.796 g of Darvan 821A dispersant (0.32 wt% based on oxides), 100.0 g of powder and ~1.2 liters of water were stirred on a stir plate for five minutes, sonicated in an ultrasonic water bath for 10 minutes, then stirred on a stir plate for about one minute.
- The slurry was poured into a 4 liter graduated cylinder containing 2.2 liters of water with a water rinse of the slurry container to reach a total volume of 3.5 liters.
- The slurry was stirred in the graduated cylinder for one minute with a long spatula, and the suspension allowed to settle, undisturbed, for four minutes.
- The supernatant was pumped from the graduated cylinder, first at 49 rpm, then at 75 rpm (Easyload Masterflex Cole Parmer pump with pump head Model 7529-10, pump drive Model 7583-50 and Tygon tubing 6408-73).
- The remaining particulates were transferred from the graduated cylinder to a 500 mL glass jar with water rinses for a final volume of ~380 mL. The supernatant was removed (estimated at 300 rpm using a Cole Parmer Pump Model 7523-20, Cole Parmer Pump Head Model 7518-10, Tygon tubing 6409-25) and the remaining powder “washed” three times with 100 mL aliquots of water (the suspension shaken and allowed to settle < 25 seconds prior to pumping off the supernatant).
- The powder was dried for 2.4 hours at 184°C. A quantity of 24.7 g powder was collected (~24.7% of the initial amount of powder used).

Powder TSP-60 was synthesized at 0.5% excess Pb with a Zr/Ti ratio of 95.7/4.3. The post-synthesis processing conditions consisted of vacuum filtration of the powder in two 24 inch diameter filters (lined with Whatman No. 3 ashless filter paper) overnight followed by oven-drying for 55 hours in ten Pyrex trays (88°C, oven as described for TSP-59). The pyrolysis, ball-milling and calcining conditions used for this powder were the same as described for TSP-46. The fractionation of this powder is outlined below:

- A mixture of 1.524 g of Darvan 821A dispersant (0.40 wt% based on oxides), 151.2 g of powder and ~1.2 liters of water were stirred on a stir plate for ~ 5 minutes, sonicated in an ultrasonic water bath for ~ 10 minutes, then stirred on a stir plate for 1 minute.
- The slurry was poured into a 4 liter graduated cylinder containing 2.2 liters of water with a water rinse of the slurry container to reach a total volume of 3.5 liters.

- The slurry was stirred in the graduated cylinder for one minute with a long spatula (could not reach the bottom 1.5 inch of the cylinder), and the suspension allowed to settle, undisturbed, for 4 minutes.
- The supernatant was pumped from the graduated cylinder, first at 47 rpm, then at 83 rpm as described above for the fractionation of TSP-59. Approximately 20-30 ml of slurry remained in the graduated cylinder.
- The remaining particulate/slurry was transferred to a 500 ml glass jar with water rinses to a total volume of ~380 ml. The supernatant was removed (pump equipment description as shown for TSP-59 fractionation) and the remaining powder “washed” three times with 100 mL aliquots of water (the suspension shaken and allowed to settle < 1 minute prior to being drawn off by pumping with equipment described earlier).
- The powder was dried for 2.3 hours at 177°C. A quantity of 36.9 g powder was collected (24.4% of the initial amount of powder used).

Results and Discussion

Study #1: Comparison of SP and TSP Produced Powders

Particle size distributions for three TSP batches and four SP16 batches are shown in Figure 1. The figure illustrates the differences between PSDs of calcined PNZT powder prepared on different scales (i.e., the presence or absence of particles > ~10 μm in size, in TSP and SP powders, respectively). To characterize the large size portion PSD “tail” of a representative TSP powder batch, powder fractionation was done using powder from TSP-46 (black curve in Figure 1). For comparison, an SP powder was also subjected to the same fractionation process as TSP-46. Although large particle size distribution tails are not apparent in the SP powders (Figure 1), there may be a small quantity of large particles in the powders that are not detectable when the powders are analyzed in the as-prepared state. Fractionation and subsequent PSD analyses were accomplished to resolve this issue. SP16O powder was chosen for this study as it was prepared using nominal baseline processing conditions within the SP16 powder series (green curve in Figure 1). The goal of the fractionation work was to isolate the portion of the powder with a particle size (equivalent spherical diameter) > ~10 μm . The isolated fractions were then characterized to determine if the microstructure, homogeneity or composition of the isolated fractions differed from those of the bulk powders.

An overlay of the PSD plots for the large, middle and fines-size fractions of TSP-46 and the non-fractionated powder is shown in Figure 2. Reasonable particle size separation was achieved for the three size fractions. Consistency in the PSD data is shown by the fact that the three size fractions encompass the entire distribution range of the non-fractionated TSP-46 powder. The large-size fraction corresponds well to the tail seen in the non-fractionated powder PSD. Approximately 50 volume % of this fraction

correspond to the $> \sim 10 \mu\text{m}$ distribution tail of the original powder. The data show that, as expected, there has been a significant concentration of the large particles in this fraction.

Less distinct size fraction separation was obtained with the SP16O fractionation experiment (Figure 3). Although the volume fraction of particles is very small, the PSD data for the middle and large fractions show the presence of these larger particles. The volume fraction for the tail is largest for the large-size fraction, which is consistent with the fractionation process. The data indicates that the SP16O powder does indeed have particles in this tail range, but the volume percent is such that this fraction is not readily detected using the standard sample preparation method for PSD analyses. The size range of particles in the distribution tail is about 10 to 40 μm as compared to 10 to 100 μm for TSP-46 (Figure 2).

SEM photomicrographs of the fines-size and large-size fractions of TSP-46 are shown in Figure 4 (loose powder sample preparation). The fines-size fraction appears to consist of mainly submicron primary particles (Figure 4a). The large-size fraction is comprised of agglomerates of the much smaller primary particles (Figure 4b). At a lower magnification, the rounded morphology of the large-size fraction agglomerates is shown (Figure 5). The rounded structure of the agglomerates may be a result of the attrition of primary particles that occurred during the post-pyrolysis ball milling operation. For comparison, the fines-size fraction of SP16O is shown in Figure 6. The primary particles in powders SP16O and TSP-46 appear to be equivalent (compare Figs. 4a and 6).

Study #2: Large-Scale Fractionation of TSP-46

A second, larger scale fractionation was performed on TSP-46 to obtain sufficient material for a more detailed analysis of the large agglomerates that make up the distribution tail. The large-size fraction of the fractionated TSP-46 powder was analyzed for PSD using two methods.

PSD Analysis of the Large-Size Fraction as a Powder

The sample preparation for the first analysis involved adding the large-size fraction powder directly into the Coulter sample cell (containing $\sim 125 \text{ mL}$ water) as a loose powder in contrast to the samples that were prepared as a slurry (sonicated in water with a dispersant). The PSD plots (Figure 7) show a bimodal distribution with mean peak diameters in the 50-60 μm range and at $\sim 3 \mu\text{m}$. The volume fraction of the 3 μm peak increased in size as the analysis progressed to the third run (the same “powder aliquot” of sample is stirred in the Coulter LS230 sample cell, with ~ 7 minutes elapsing for 3 runs). Correspondingly, the 60 μm peak decreased in size. This indicates that the powder particles in this as-dispersed state were relatively fragile and broke up during analysis due to the agitation in the Coulter sample cell. This was confirmed by the increase in the obscuration value measured by the Coulter instrument (increasing from 63 to 86% over three runs; a typical change in obscuration is in the range of 3-4%). Obscuration is the

percentage of laser light that is scattered by the sample particles, i.e., the more particles present, the more light is scattered and the higher the obscuration value.

PSD Analysis of the Large-Size Fraction as a Slurry

To evaluate the strength of the agglomerates in the large-size fraction, a second series of analyses were performed in which PSDs were determined as a function of slurry sample sonication time. The sample sonication times were 3 minutes (the standard sample sonication time for routine analyses), 10, 15, and 30 minutes, with a new slurry prepared for each sonication time. Figure 8 shows the PSD overlays of runs at these four sonication times (also includes the PSD of the non-fractionated powder). With increasing sonication times, the peak at $\sim 40\text{-}50\text{ }\mu\text{m}$ decreases in size, though the overall distribution range covered the range of the non-fractionated TSP-46 powder (purple curve). It is thought that, with increasing sonication time, the larger particles (see Figure 5), continue to breakdown, increasing the number of smaller-fragment particles and even smaller primary particles shown in Figure 4a. The mean particle diameter and volume percent of particles $> \sim 10\text{ }\mu\text{m}$ as a function of sonication time are shown in Table 1. After 30 minutes of sonication time, the equivalent volume percent of particles $> \sim 10\text{ }\mu\text{m}$ for the large-size fraction approaches that of the non-fractionated powder (10.9 volume percent vs. 8.1 volume percent).

Table 1. Particle Size Results for Large-Size Fraction and Non-fractionated TSP-46 Powder as a Function of Sonication Time.

TSP-46 Sample Description	Particles $> \sim 10\mu\text{m}$ (Volume %)	Mean Particle Diameter (μm)
Large-size fraction, 3 min sonication	41.6	16.5
Large-size fraction, 10 min sonication	28.6	10.6
Large-size fraction, 15 min sonication	21.9	7.29
Large-size fraction, 30 min sonication	10.9	4.46
Non-fractionated, 3 min sonication	8.1	5.11

SEM photomicrographs of TSP-46 were obtained from powder suspensions deposited onto SEM stubs coated with adhesive tape (Figures 4-6). To further characterize the structure of the large agglomerated particles, powder from the large-size fraction of TSP-46 was encapsulated and polished to obtain particle cross-sections. Figure 9 is presented to illustrate the rounded nature of the agglomerated particles. In the agglomerates, the PZT primary particles are packed together with varying density and contain zirconia-rich islands as seen by examining Figure 10. At the higher magnification, these islands are easily visible. Their origin is postulated to be from the overall powder stoichiometry being deficient in lead. This deficiency causes zirconia to preferentially segregate into islands.

Study #3: Effects of Large Particles on Sintering

Information on the structure and strength of the particles that make up the $> \sim 10 \mu\text{m}$ tail of the TSP powder particle size distribution have been discussed. The final aspect of the $> \sim 10 \mu\text{m}$ portion of the PSD to be documented here deals with its chemical composition and sinterability. As previously described in the experimental section, two TSP powders (TSP-59 and -60) were examined. The main processing difference between TSP-59 and -60 was the time and the method the batches were filtered after chemical synthesis. Batch TSP-59 was dried in the vacuum filter for six days, while TSP-60 was dried in the filter for only one day (see Experimental Section for details) prior to oven drying. Also, the filter cake for TSP-59 was broken up several times over the six day time period. The two batches were chosen for this study to determine if this filtering/drying difference had any effect on the properties of the PSD tail. Also, a new drying oven was added to the TSP production-scale process beginning with batch TSP-54 to accommodate the wetter filter cakes that result when the one-day filtering operation is used, so a comparison to powder TSP-46 was desired. Therefore, batch TSP-59 is representative of the pre-production PNZT material (TSP-46) being made at this time by the TSP process.

The particle size distributions of non-fractionated TSP-59 and -60 powders are shown in Figure 11. The distributions for the powders are very similar, with both having the $> \sim 10 \mu\text{m}$ distribution tail. Based on the particle size distributions, the effect of one-day filtration versus six-day filtration appears to be insignificant. Also, a comparison of these PSDs with the TSP distributions given in Figure 1 (much earlier TSP runs; former precipitate-drying oven) show that the particle size distributions of the newer powders are similar to the powders from the older batches.

TSP-59 and TSP-60 powders were fractionated as described in the Experimental Section. For comparison with TSP-46, SEM photomicrographs of polished cross-sections of the agglomerates from the large-size fractions are given in Figures 12 and 13 (TSP-59) and Figures 14 and 15 (TSP-60). From the figures it is seen that the structure of the agglomerates is very similar for all three of the TSP batches. All are composed of mainly submicron PNZT primary particles that are assembled into regions of varying density and all contain zirconia-rich islands. These islands are often surrounded by PZT “shells.” These shells are a commonly seen feature in the chem-prep powder microstructures.

Compositional analyses were performed to determine if the stoichiometry of the large agglomerates ($> \sim 10 \mu\text{m}$) found in the TSP powders differed from the bulk composition of the non-fractionated powder. Using Inductively-Coupled Plasma Atomic Emission Spectroscopy (ICP-AES), the mole fractions of Pb, Nb, and Zr (expressed as a fraction of the total of Zr and Ti) of the large particle size fractions obtained from TSP-59 and TSP-60, along with the those of the non-fractionated powders, were determined. Duplicate samples were run for each powder and three measurements were made on each sample (the average values for each sample are given in Table 2). It should be noted that the fractionation process was not completely efficient in producing samples that contained only the large particles that made up the $> \sim 10 \mu\text{m}$ tail of the PSDs. Based on results

from the fractionation of TSP-46, between 40 and 50% of the large-size fraction samples were from the $> \sim 10 \mu\text{m}$ tail of the PSD (see 3 minute sonication data given in Figure 8). Therefore the ICP results are not completely conclusive because more than just the $> \sim 10 \mu\text{m}$ fraction of PSD was analyzed.

Table 2. ICP Results for Non-fractionated and Large-size Fractions of TSP-59 and TSP-60.

Batch ID	ICP CAL. Ref. No. ¹	% Zr in (Zr + Ti) ²	% Ti in (Zr + Ti)	Nb mole fraction	Pb mole fraction
TSP-59	02001-2	95.49	4.51	0.0178	0.9436
TSP-59	02034A	95.46	4.54	0.0180	0.9691
TSP-59L-1	02034A	95.43	4.57	0.0180	0.9701
TSP-59L-2	02034A	95.44	4.56	0.0180	0.9664
TSP-60	02001-2	95.70	4.30	0.0179	0.9428
TSP-60	02034A	95.70	4.30	0.0179	0.9408
TSP-60L-1	02034A	95.67	4.33	0.0180	0.9639
TSP-60L-2	02034A	95.67	4.33	0.0181	0.9569

¹The non-fractionated powders were analyzed on two different days (noted by different CAL. Ref. No. shown in the table); the large-size fractions were analyzed in duplicate in one analysis (CAL02034A, referred to as “L-1” and “L-2”). ²Targeted mole fractions were as follows: Zr – 95.7, Ti – 4.3, Nb – 0.0180, and Pb – 0.996. The low Zr value for TSP-59 is thought to be due to a weighing error during synthesis.

The ICP results, as given in Table 2, show that within each TSP sample set (e.g., TSP-59 and TSP-59L, or TSP-60 and TSP-60L), the average Nb values are very consistent between the non-fractionated and the large-size fractionated powders. (See Figures 16-19 for plots of the 95% confidence intervals for the average values of Pb, Nb and Zr measured for each powder). From Table 2, it appears that there is a slight decrease in Zr content for the large-size fraction over the non-fractionated TSP-59 and TSP-60 powders, however, since the confidence intervals for average Zr content overlap, no distinction can be made between the powders’ Zr content. Similarly for the Pb results, the error in the triplicate measurements (leading to wide confidence intervals) makes it impossible to distinguish the fractionated from the non-fractionated powders. More ICP analyses would be required to determine if the fractionated and non-fractionated powders possess different stoichiometries, and since the fractionation process itself is not completely efficient as noted earlier, it has been deemed unfeasible to pursue this at this time.

To evaluate the effect of large-size fraction (agglomerated) TSP-59 and -60 powders on microstructure, each powder was incorporated into slugs using a “sandwich configuration” and sintered (Figure 20). The two fractions, having no binder or pore former, were layered between a blend of TSP’s -39, -40, and -46 and sintered at 1350°C for 6 hours. SEM photomicrographs of polished cross-sections of the large-size fraction layers of TSP-59 and -60 are shown in Figures 21 and 22. One can see a greater concentration of larger, more distinct pore clusters in the TSP-59 layer than in the TSP-60 layer (Figure 21). In addition, clusters in the TSP-59 layer are noticeably more porous (Figure 22) than those in the TSP-60 layer.

Once formed, hard agglomerates or portions of the agglomerates can persist throughout powder processing and, if not fragmented during milling operations, preferentially sieved, or crushed during powder compaction, can evolve into regions of high porosity

that are difficult to eliminate during sintering. Depending on powder processing conditions, the microstructure of PZT 95/5 may contain inhomogeneities, such as, pore clusters. The extent of porosity within a pore cluster can vary. For example, the cluster porosity can vary from slightly open to a very open pore structure (Figure 22).

Similar to the large-size fraction powders, non-fractionated TSP-59 powder (six-day vacuum dry during post-synthesis processing) has more of the larger pore clusters than the non-fractionated TSP-60 powder (Figure 23). Further, the degree of porosity within the pore clusters is similar when comparing large-size fraction and non-fractionated samples. (The large circular pores seen in the slugs made from non-fractionated powder in Figure 23 are due to the Lucite pore former added during powder processing. The pore former was not used in the large-size fraction layers, Figures 21 and 22.)

Though a limited number of samples were examined, it should be noted that the large-size fraction of TSP-59 appears to have a greater concentration of the large, more porous clusters than the non-fractionated TSP-59 sample (slugs 30 and 35 in Figures 21 and 23, respectively). This suggests that the large-size fraction contains more agglomerates per volume than the non-fractionated powder, thus there is a higher concentration of pore clusters in the large-size fraction powder. However, this is not the case for the large-size fraction of TSP-60, which appears to have a similar concentration of pore clusters when compared to the non-fractionated TSP-60 sample (slugs 41 and 50 in Figures 21 and 23, respectively).

For comparison, two additional slugs were examined. These slugs, prepared from powders TSP-58 and TSP-61, are replicates of powder batches TSP-59 and TSP-60, respectively, in that post-synthesis processing conditions were the same. Figure 24 shows SEM photomicrographs of TSP-58 (processed the same as TSP-59, six-day vacuum dry) and TSP-61 (processed the same as TSP-60, one-day vacuum dry). Again, the powder processed with a six-day vacuum dry (TSP-58) contained a higher concentration of porous regions than the one-day vacuum dry sample (TSP-61). Possibly, the larger, more distinct pore clusters observed in the six-day dry specimens (TSP-58 and -59) result from the longer drying time. As shown in Figure 23, the large circular pores found in the non-fractionated slugs in Figure 24 result from the Lucite pore former that was used.

In addition to pore clusters, zirconia-rich regions have also been observed in sintered PNZT 95/5 (Figure 22). As with pore clusters, this second phase is potentially detrimental to the electrical, mechanical and functional properties of PNZT 95/5. A study is currently being undertaken to address the origin of the pore clusters and zirconia-rich regions and to determine what effect, if any, they have on the mechanical and functional properties of PNZT 95/5.

It should be noted that explosive functional test results for the TSP batches used in this study (one-day dry: TSP-60 and TSP-61; six-day dry: TSP-58) were similar at the cold test condition – a ~10% high voltage breakdown rate. At the ambient test condition,

however, 1 of 2 units tested using voltage bars prepared from the six-day dried material broke down, while 10 of 10 units tested passed for the one-day-derived material.

Conclusions

In conclusion, this SAND report has documented the characteristics of the large particle size fraction ($> \sim 10 \mu\text{m}$) that is typically found in TSP-prepared PZT 95/5. These particles have been identified as being very similar in structure and composition as the bulk powder. They are agglomerates of submicron primary PZT particles, porous PZT aggregates, and dense zirconia-rich particles that tend to be coated with a PZT shell. The large particles are broken down with time when slurried and sonicated to particles with sizes similar to that of the $< \sim 10 \mu\text{m}$ portion of the bulk powder's PSD. Compositional analyses of the large-size fraction and the non-fractionated powders were inconclusive.

Sintering studies have shown that the large-size fractions of the TSP powders behave similarly to the sintered non-fractionated powder with respect to the types of microstructural features found. The six-day dried material had more, well-defined porous inclusions than the one-day dried material. Also, the six-day dried large-size fraction had a higher concentration of porous regions than its respective non-fractionated powder. This was not observed in the one-day dried material (large-size fraction vs. non-fractionated powder). Implications of the one-day versus the six-day drying time with respect to functional test performance are difficult to answer based on the limited number of powder batches and FTU's tested. However, because high reliability is critical, a $\sim 10\%$ FTU failure rate is unacceptable. More insight into performance-related issues with respect to microstructure will hopefully be developed as more TSP lots are processed, tested and characterized.

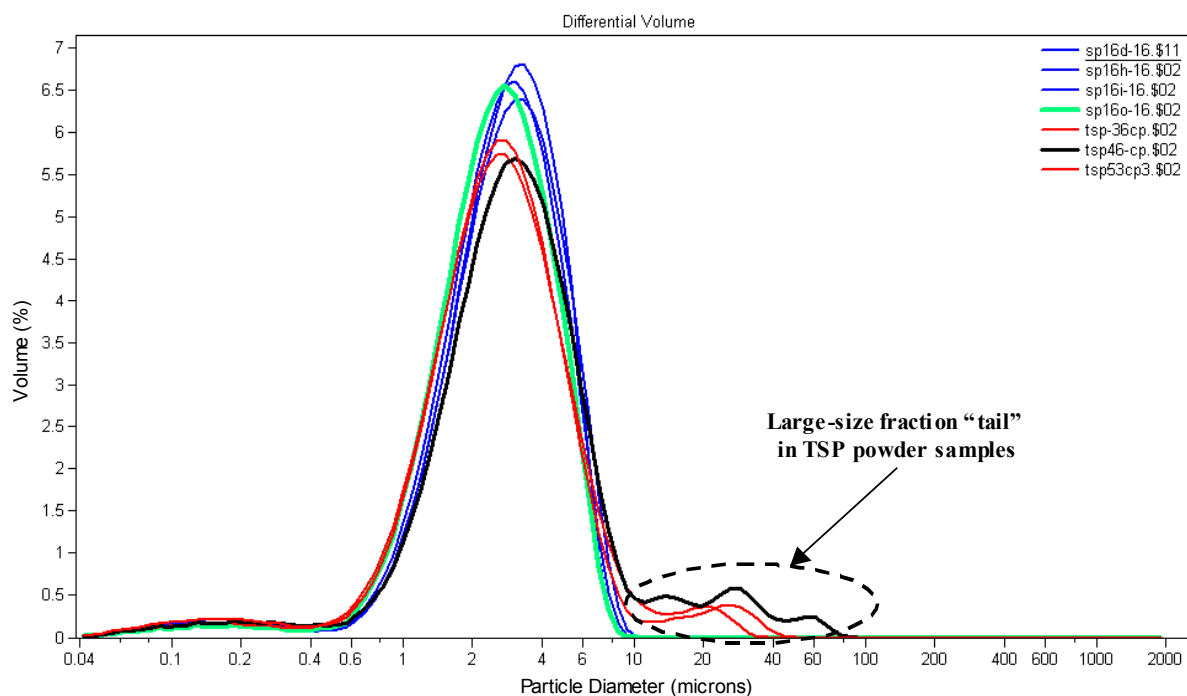


Figure 1. Comparison of PSD of SP16 Series powders to TSP Center Point (CP) batch powders.

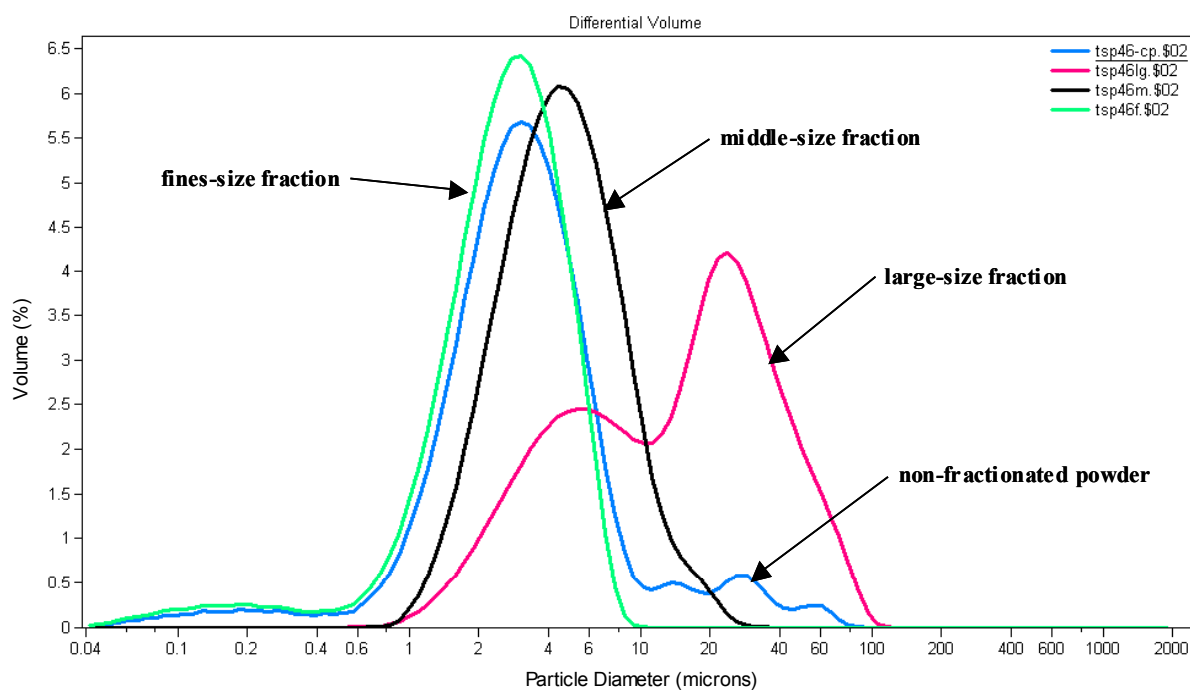


Figure 2. Overlay of PSD curves for three size fractions of TSP-46 compared to the non-fractionated TSP-46 powder.

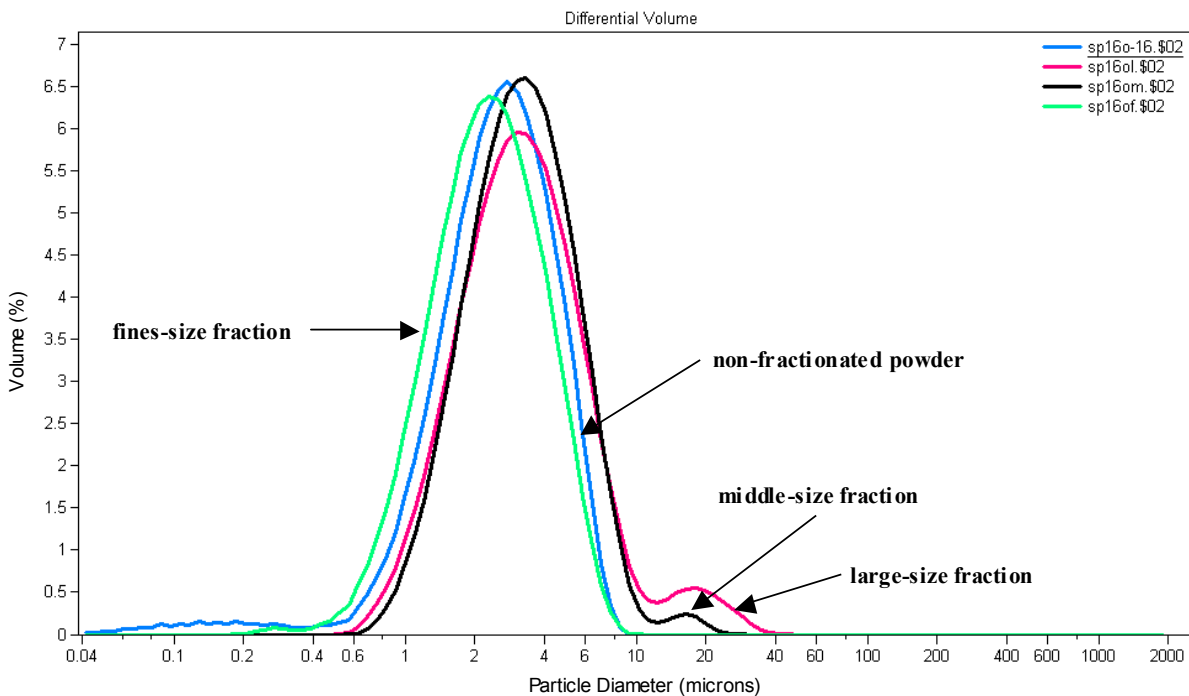
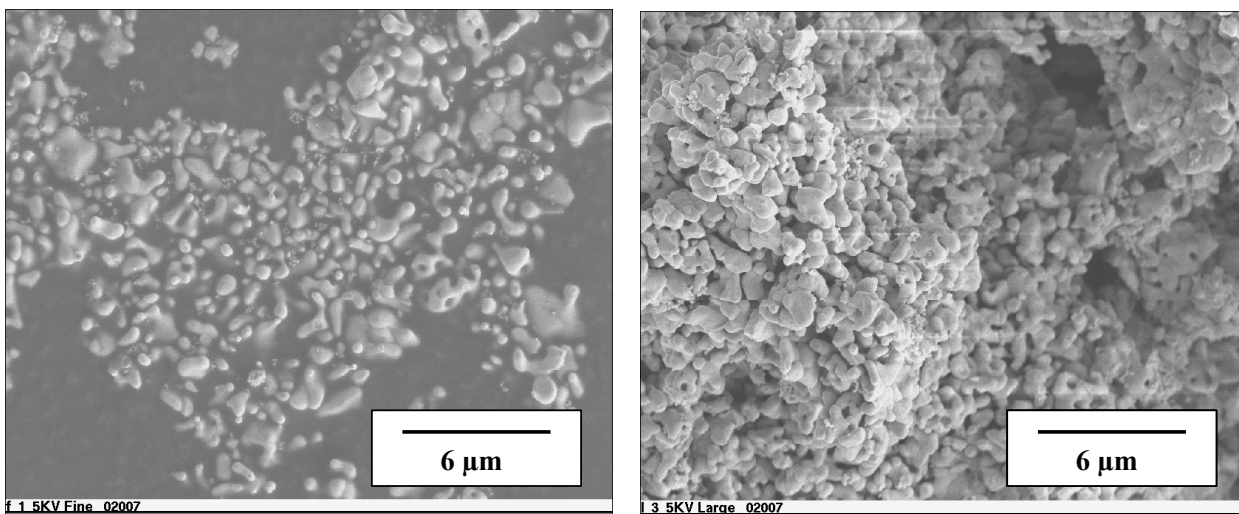


Figure 3. Overlay of PSD curves for three size fractions of SP16O compared to the non-fractionated SP16O powder.



4a) “Fines-size Fraction”

4b) “Large-size Fraction”

Figure 4. SEM photomicrographs of: a). TSP-46 fines-size fraction shows primary PZT particles. b). TSP-46 large-size fraction is comprised of agglomerates of primary PZT particles.

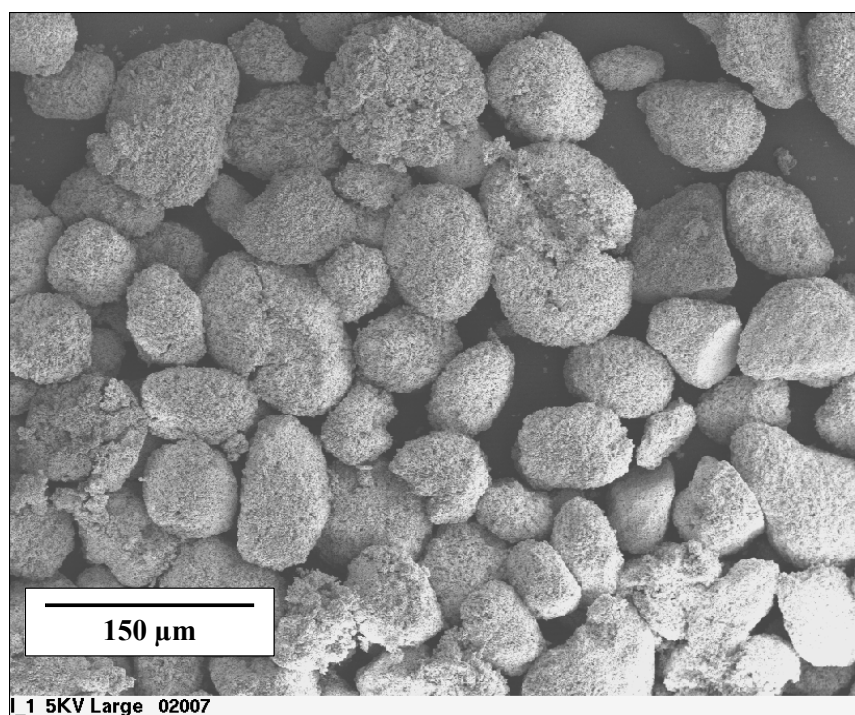


Figure 5. SEM photomicrograph of large-size fraction of TSP-46 showing the rounded morphology of the agglomerates that are comprised of the sub-μm PZT primary particles.

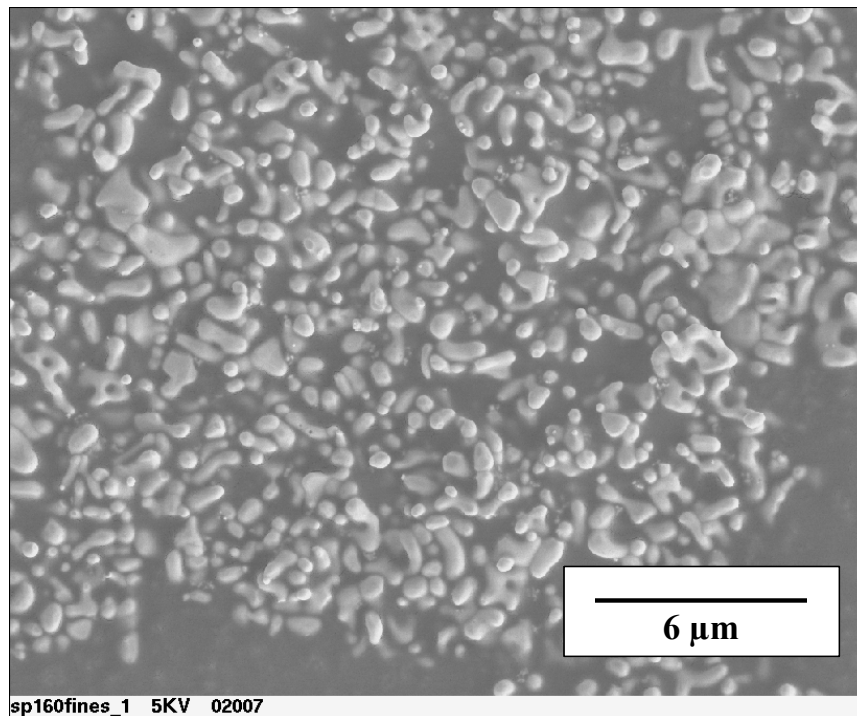


Figure 6. SEM photomicrograph of fines-size fraction of SP16O showing PZT primary particles equivalent to those seen in the fines-size fraction of TSP-46.

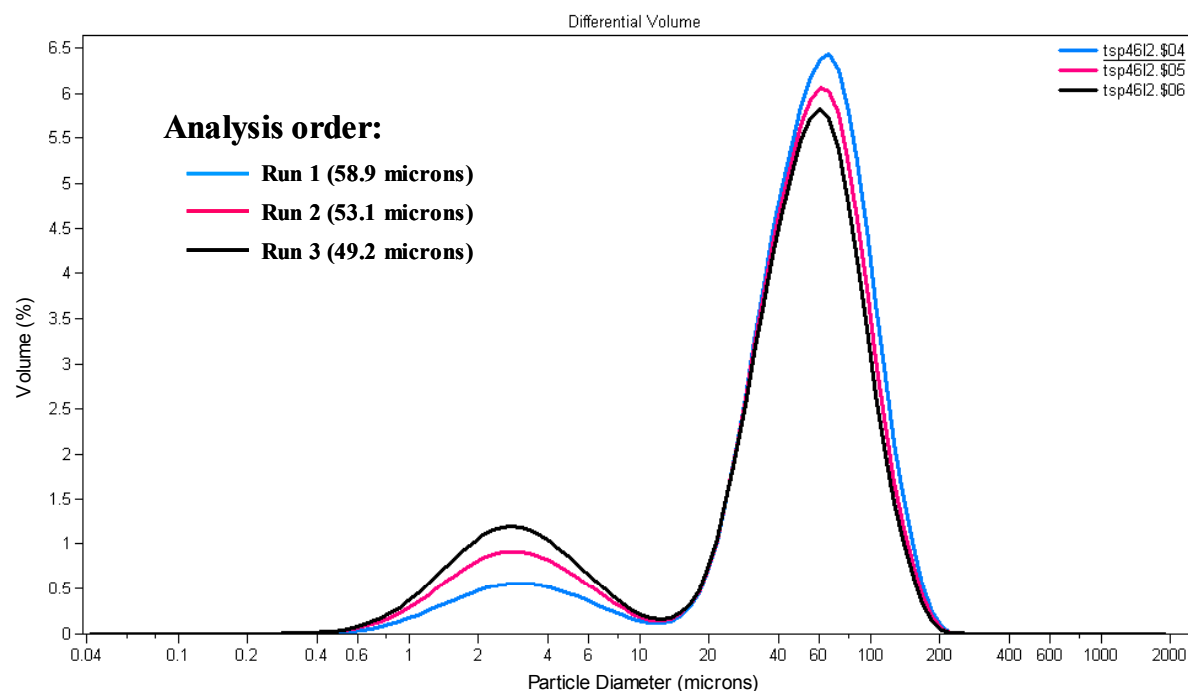


Figure 7. Particle size distribution data of TSP-46 large-size fraction analyzed as a powder rather than as a slurry. Approximately 7 minutes elapsed over the course of the three runs in the Coulter LS230 cell. Listed for each run is the mean particle size in microns.

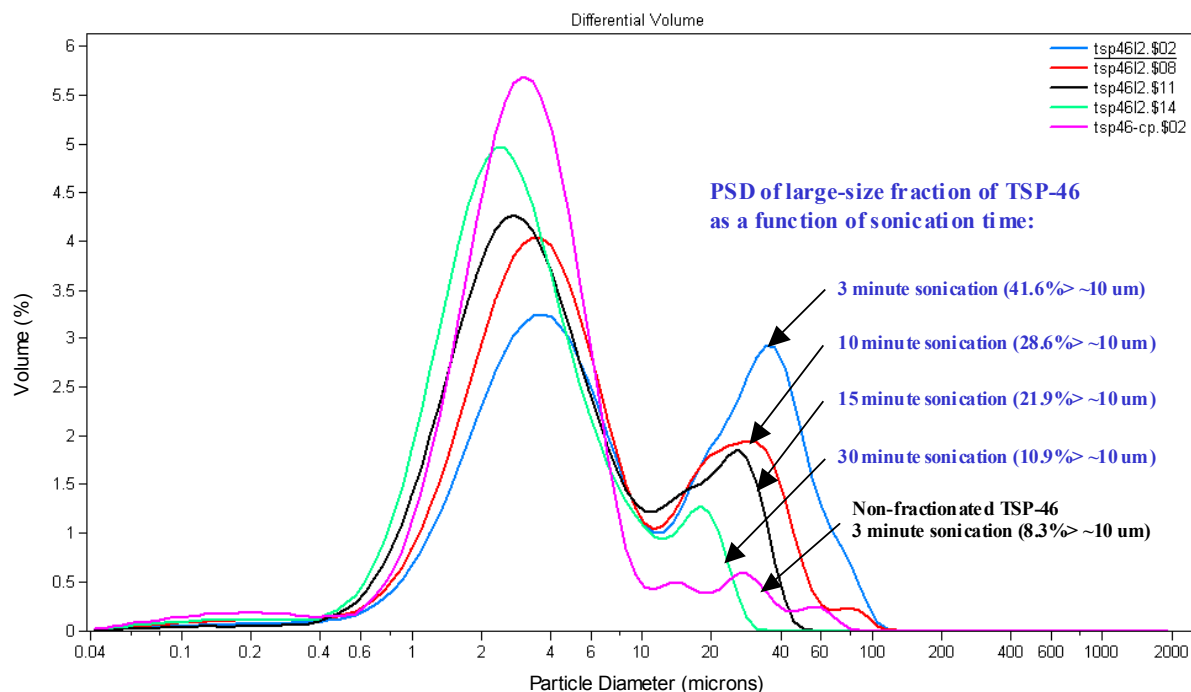


Figure 8. PSD overlays of TSP-46 large-size fraction as a function of increasing sonication times of slurry sample prior to particle size analysis. Also shown is the PSD for the non-fractionated powder.

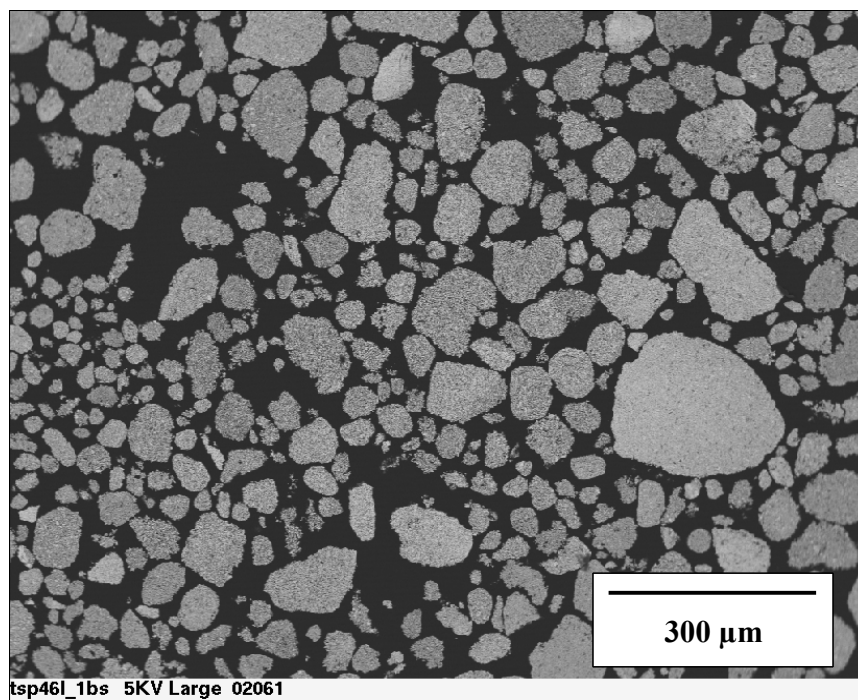


Figure 9. SEM photomicrograph of agglomerate cross-section of encapsulated and polished loose powder from large-size fraction of TSP-46.

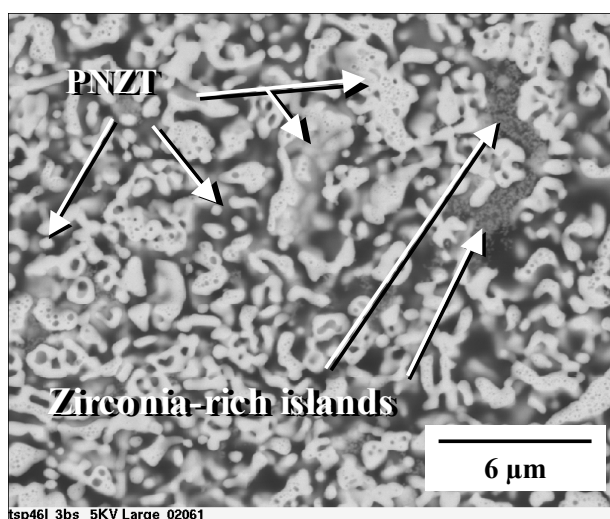
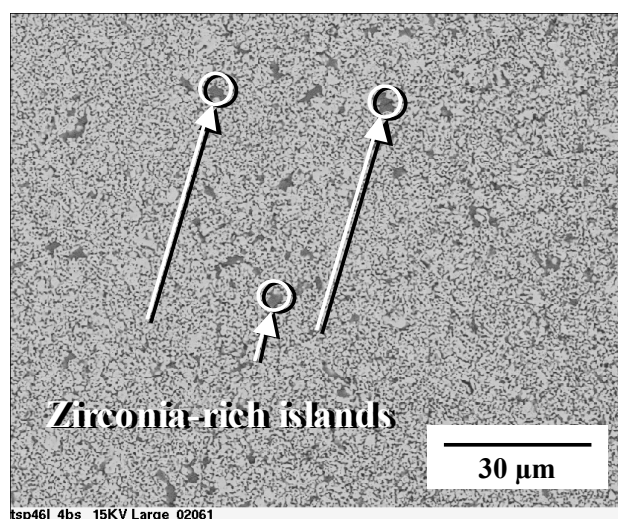


Figure 10. High magnification SEM photomicrographs of agglomerate cross-section of encapsulated and polished loose powder from large-size fraction of TSP-46.

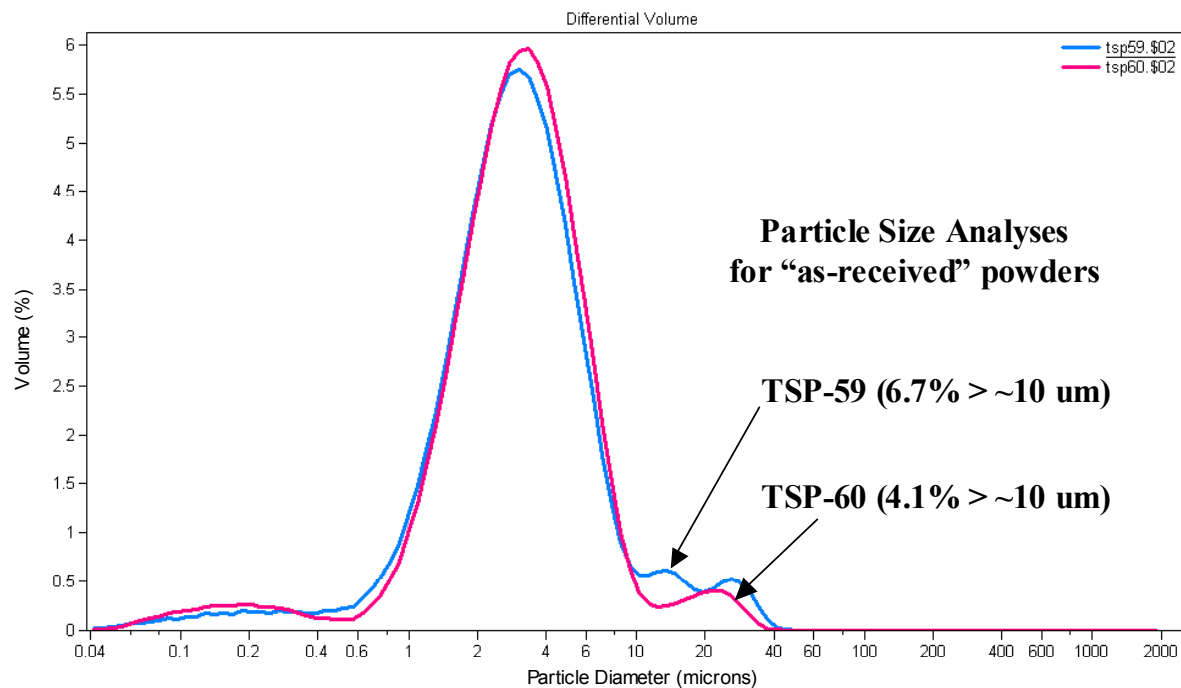


Figure 11. PSD of non-fractionated TSP-59 and TSP-60 powders showing the volume % of particles > ~10 um.

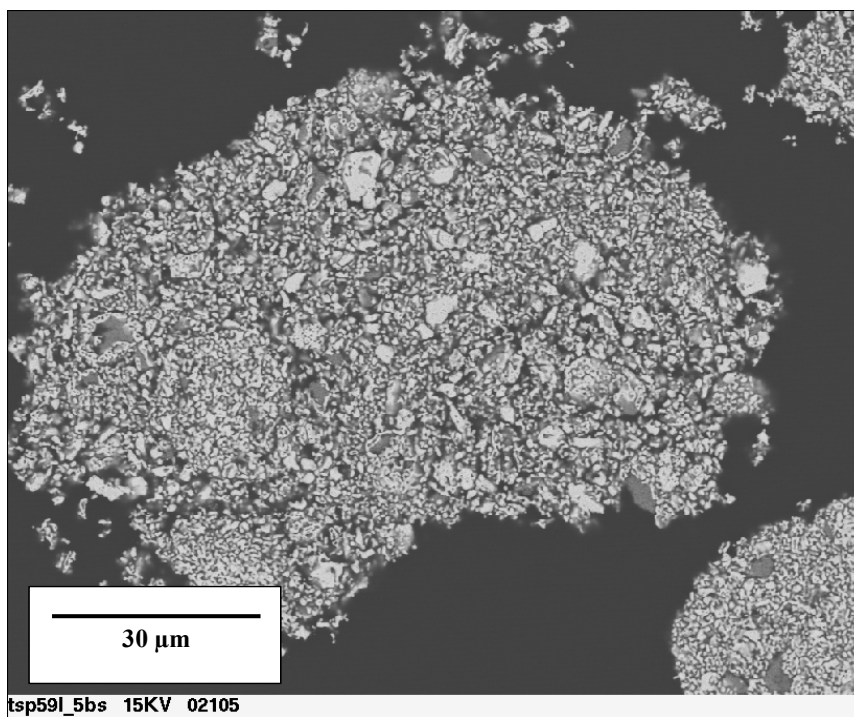


Figure 12. SEM photomicrograph of agglomerate cross-section of encapsulated and polished loose powder from large-size fraction of TSP-59.

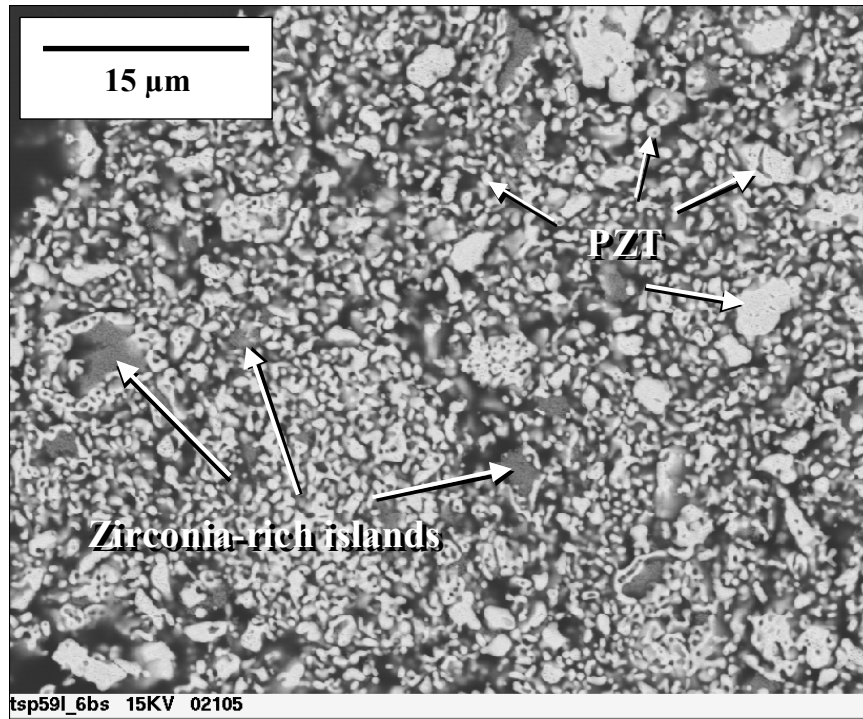


Figure 13. Higher magnification SEM photomicrograph of agglomerate cross-section of encapsulated and polished loose powder from large-size fraction of TSP-59.

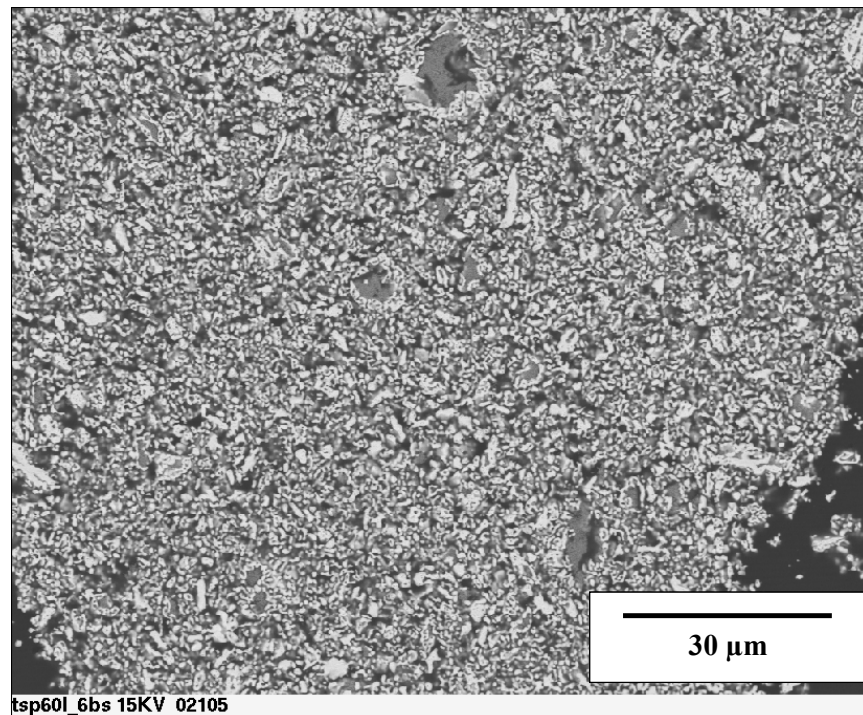


Figure 14. SEM photomicrograph of agglomerate cross-section of encapsulated and polished loose powder from large-size fraction of TSP-60.

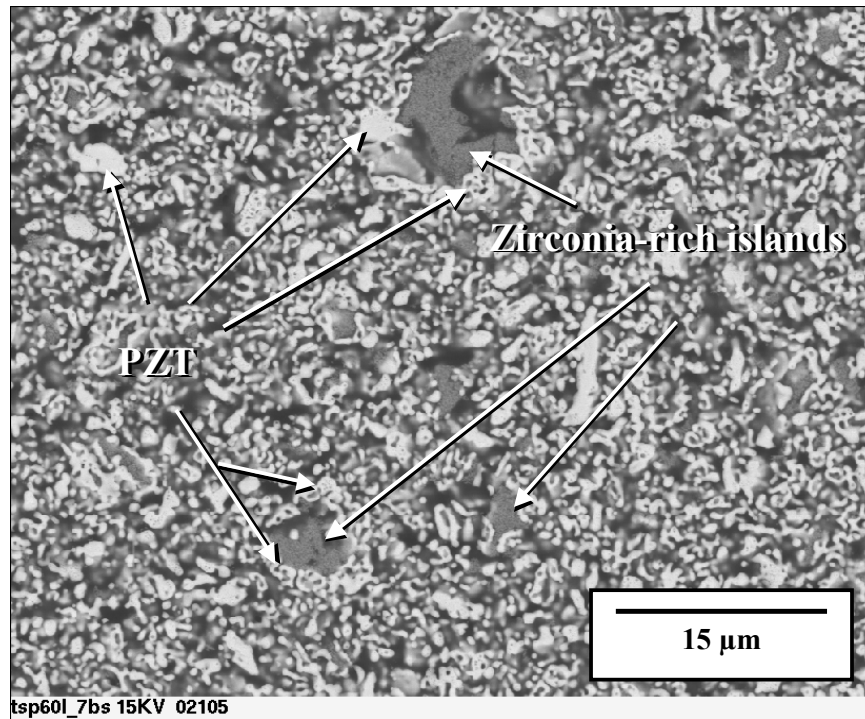


Figure 15. Higher magnification SEM photomicrograph of agglomerate cross-section of encapsulated and polished loose powder from large-size fraction of TSP-60.

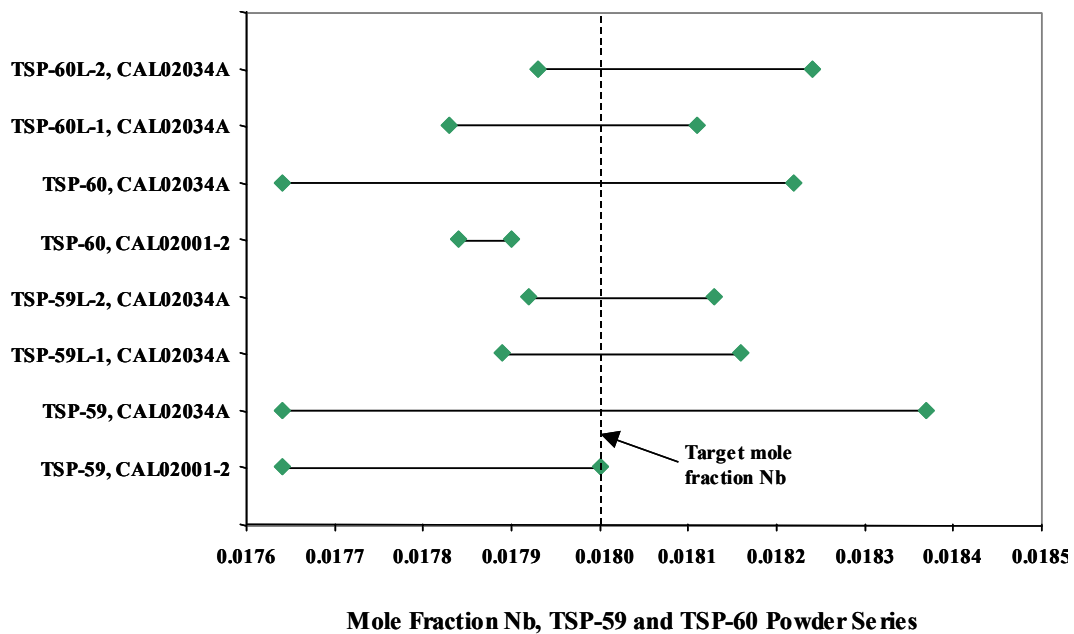


Figure 16. 95% confidence intervals for ICP compositional analyses of Nb for the TSP-59 and TSP-60 series powders.

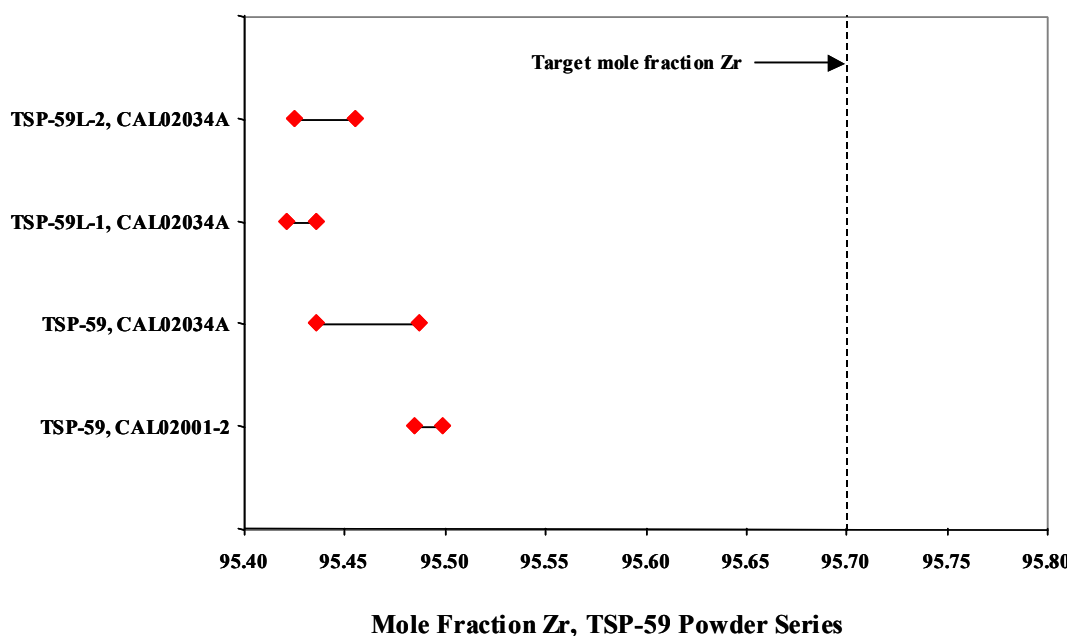


Figure 17. 95% confidence intervals for ICP compositional analyses of Zr for the TSP-59 series powders.

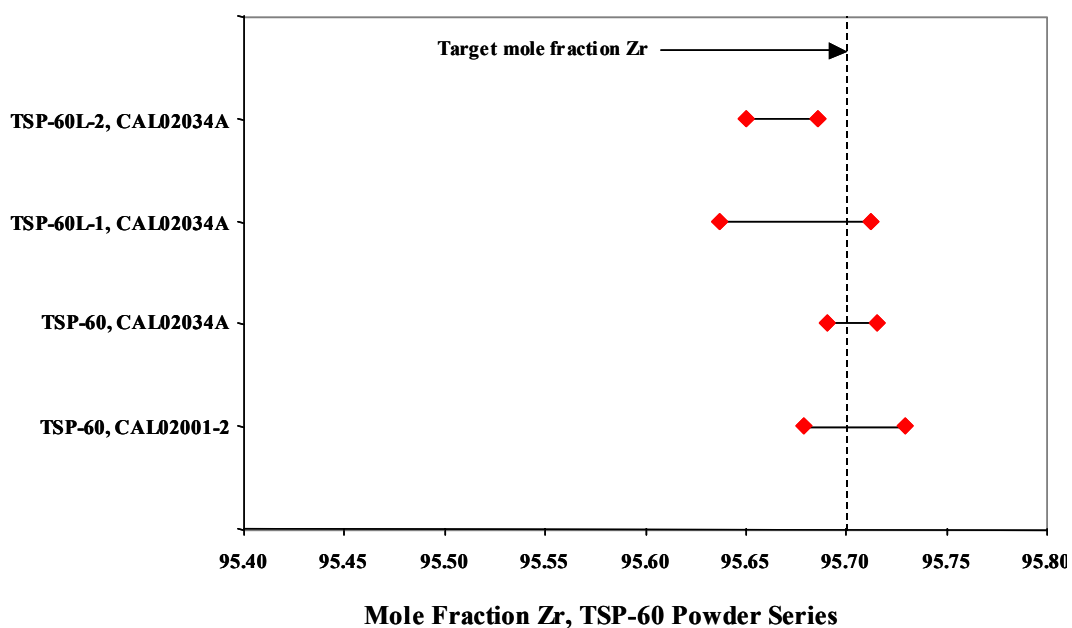


Figure 18. 95% confidence intervals for ICP compositional analyses of Zr for the TSP-60 series powders.

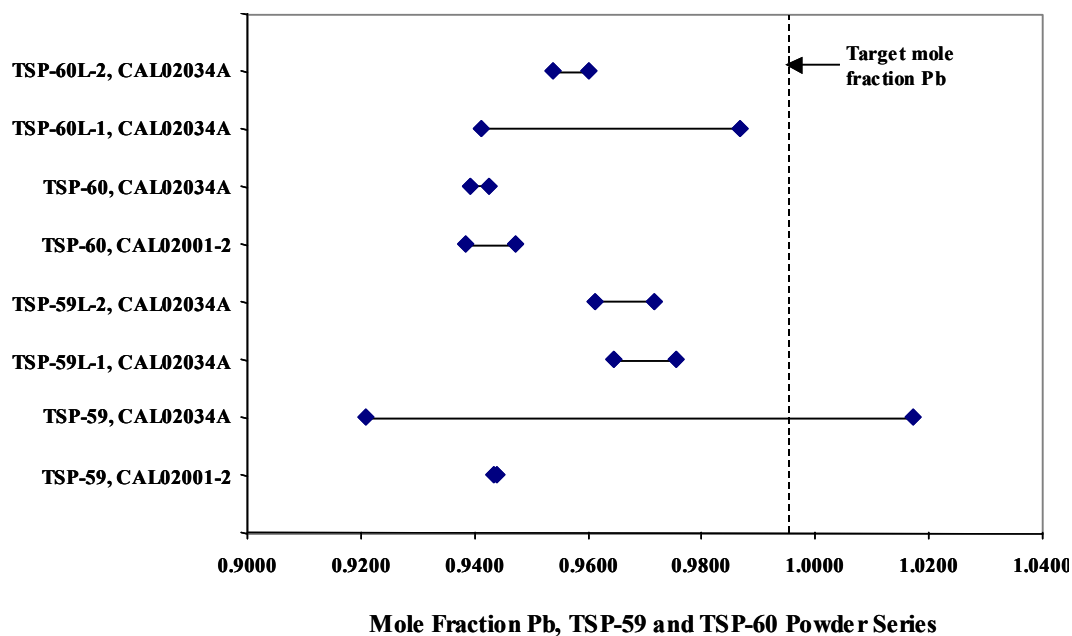
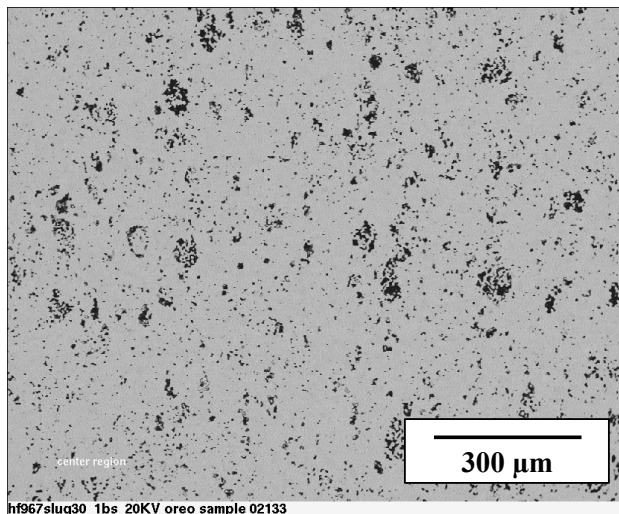


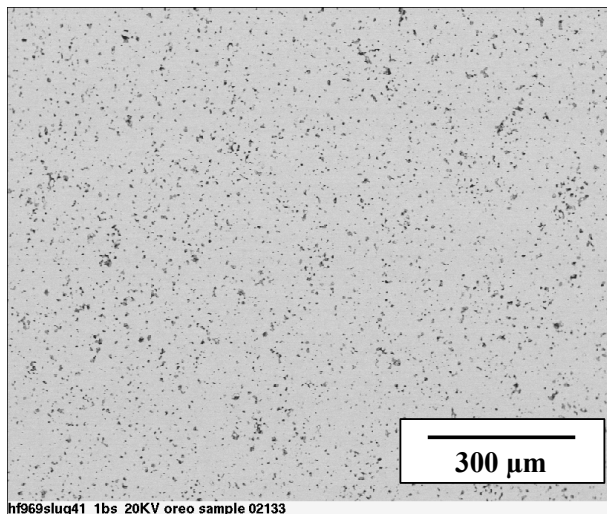
Figure 19. 95% confidence intervals for ICP compositional analyses of Pb for the TSP-59 and TSP-60 series powders.



Figure 20. Schematic to illustrate the method of layering large-size fraction powder between layers of a TSP powder blend to form a slug for high fire.

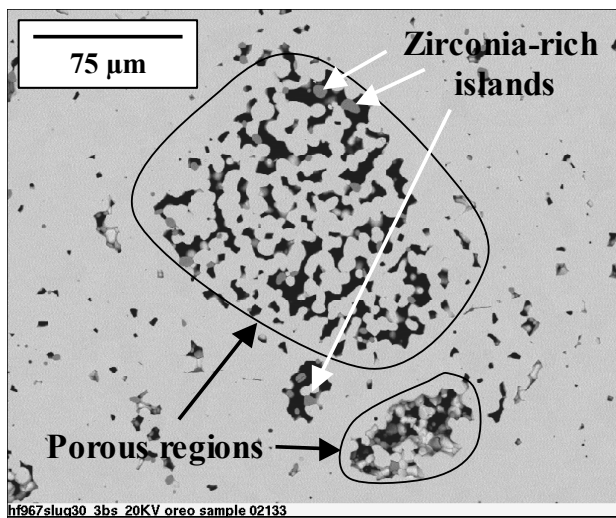


TSP-59 “Center,” HF967, Slug 30

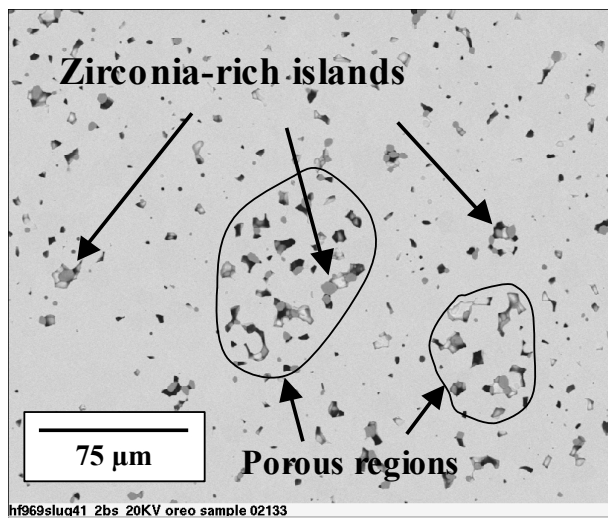


TSP-60 “Center,” HF969, Slug 41

Figure 21. SEM photomicrographs of polished cross-sections of the large-size fraction layers comprised of powders TSP-59 and TSP-60 in high fired slugs.

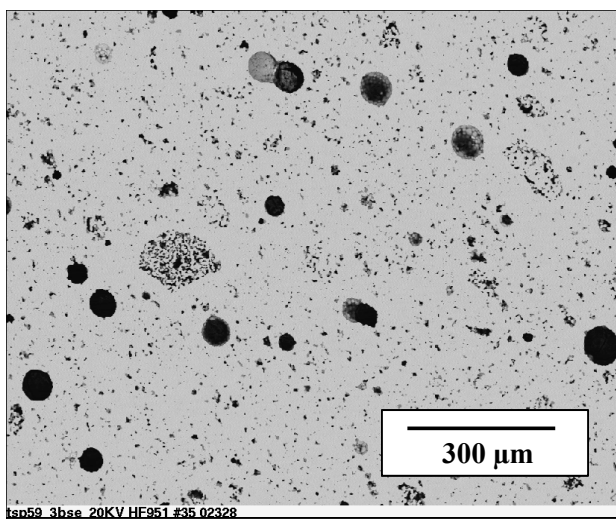


TSP-59 “Center,” HF967, Slug 30

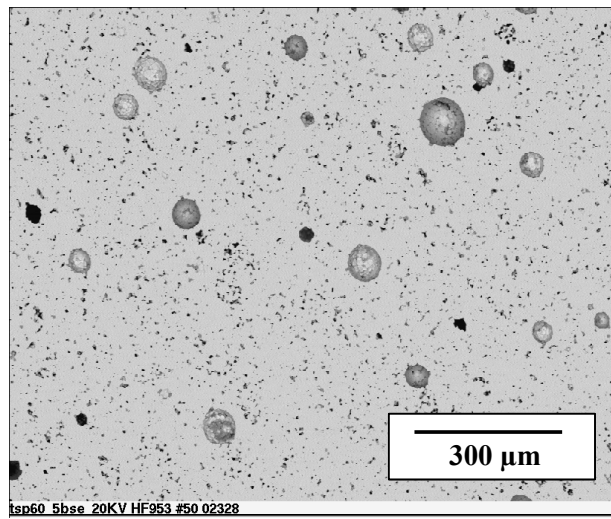


TSP-60 “Center,” HF969, Slug 41

Figure 22. Higher magnification SEM photomicrographs of polished cross-sections of the large-size fraction layers comprised of powders TSP-59 and TSP-60 in high-fired slugs.

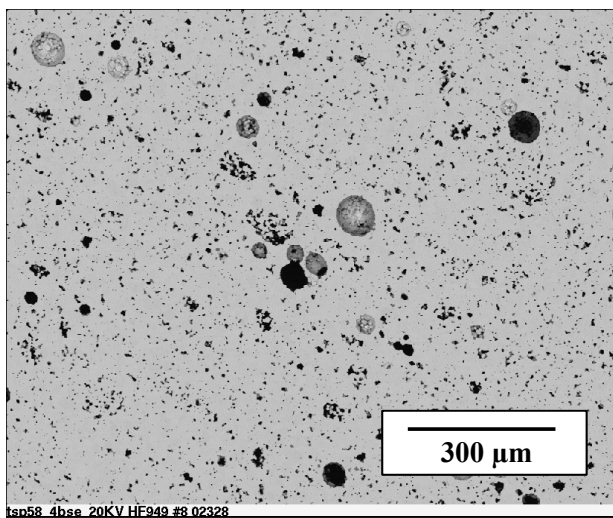


TSP-59, HF951, Slug 35

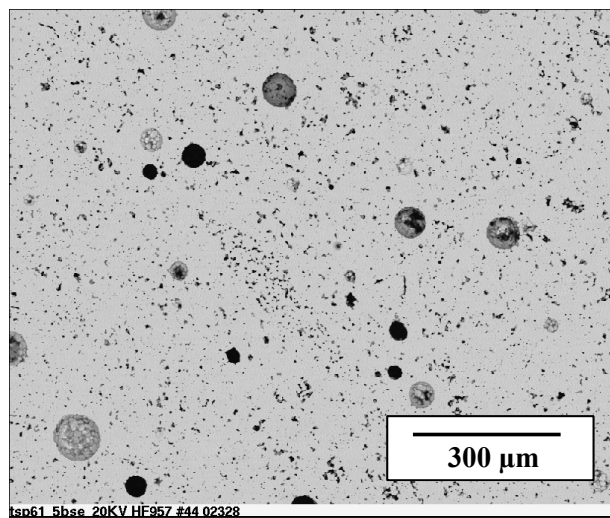


TSP-60, HF953, Slug 50

Figure 23. SEM photomicrographs of polished cross-sections of slugs prepared from non-fractionated powders of TSP-59 and TSP-60.



TSP-58, HF949, Slug 8



TSP-61, HF957, Slug 44

Figure 24. SEM photomicrographs of polished cross-sections of slugs prepared from powders TSP-58 and TSP-61. These slugs represent replicates of TSP-59 and TSP-60, respectively, as their post-synthesis processing was the same.

References

1. Voigt, J.A., Sipola, D.L., Ewsuk, K.G., Tuttle, B.A., Moore, R.H., Montoya, R.V., and Anderson, M.A., *Solution Synthesis and Processing of PZT Materials for Neutron Generator Applications*, SAND98-2750. Sandia National Laboratories, Albuquerque, NM, December, 1998
2. Sipola, D.L., Voigt, J.A., Lockwood, S.J., Rodman-Gonzales, E.D., *Chem-Prep PZT 95/5 for Neutron Generator Applications: Particle Size Distribution Comparison of Development and Productions-Scale Powders*, SAND2002-2065. Sandia National Laboratories, Albuquerque, NM, July, 2002
3. Lockwood, S.J., Rodman, E.D., DeNinno, S.M., Voigt, J.A., and Moore, D.L., *Chem-Prep PZT 95/5 for Neutron Generator Applications: Production Scale-up Early History*, SAND2003-0943. Sandia National Laboratories, Albuquerque, NM, March, 2003.
4. Moore, D.L., et al, *Chem-Prep PZT 95/5 for Neutron Generator Applications: Process Development Summary*. SAND report to be published

Distribution:

1	MS0886	J.C. Barrera, 1822
1	0886	R.P. Goehner, 1822
1	0886	B.B. McKenzie, 1822
1	0886	J.E. Reich, 1822
1	0886	P.H. Wilks, 1822
1	MS0889	S. J. Glass, 1843
1	0889	C. S. Watson, 1843
1	MS1349	K. G. Ewsuk, 1843
1	1349	W. F. Hammetter, 1843
1	MS1411	J. Liu, 1846
5	1411	D. L. Moore, 1846
5	1411	J. A. Voigt, 1846
1	MS0515	J. D. Keck, 2561
1	MS0521	T. W. Scofield, 2561
1	MS0959	T. J. Gardner, 14192
1	0959	J. T. Gibson, 14192
1	0959	J. P. Hanlon, 14192
1	0959	M. A. Hutchinson, 14192
3	0959	S. J. Lockwood, 14192
1	0959	R. H. Moore, 14192
1	0959	E. D. Rodman, 14192
1	0959	P. Yang, 14192
1	MS9018	Central Technical Files, 8945-1
2	0899	Technical Library, 9616
1	0612	Review & Approval Desk, 9612
		For DOE/OSTI